Electromagnetic Surface Modes in Structured Perfect-Conductor Surfaces

F. J. García de Abajo[1,*] and J. J. Sáenz[2]

[1]Centro Mixto CSIC-UPV/EHU and Donostia International Physics Center (DIPC), Apartado 1072, 20080 San Sebastian, Spain
[2]Departamento de Física de la Materia Condensada, Universidad Autónoma de Madrid, Cantoblanco, 28049 Madrid, Spain

(Received 3 June 2005; published 30 November 2005)

Surface-bound modes in metamaterials forged by drilling periodic hole arrays in perfect-conductor surfaces are investigated by means of both analytical techniques and rigorous numerical solution of Maxwell's equations. It is shown that these metamaterials cannot be described in general by local, frequency-dependent permittivities and permeabilities for small periods compared to the wavelength, except in certain limiting cases that are discussed in detail. New related metamaterials are shown to exhibit exciting optical properties that are elucidated in the light of our simple analytical approach.

DOI: 10.1103/PhysRevLett.95.233901 PACS numbers: 42.25.Fx, 41.20.Jb, 42.79.Dj, 73.20.Mf

Structured metal surfaces offer a playground to yield remarkable optical phenomena ranging from extraordinary light transmission through subwavelength hole arrays [1] to innovative types of surface resonances [2]. The relevant role of surface plasmons [3] at visible and near-infrared frequencies was emphasized in early developments [1,4], while subsequent studies, following pioneering works in the field [5,6], demonstrated similar effects in plasmon-free good conductor films at microwave and THz frequencies [7,8]. Recently, these two regimes have been connected by the exciting prediction of Pendry *et al.* [2] of surface resonances that mimic surface-plasmon behavior in perfect-conductor surfaces (PCSs) textured with subwavelength holes, and by its subsequent experimental observation [9].

Surface plasmons, originally predicted by Ritchie [3], have given birth to the rapidly growing field of plasmonics owing to their potential application in areas as diverse as biosensing [10], information processing via metal-surface circuits [11], or laser technology [12]. Hence the importance of devising new ways to achieve surface-plasmon-like behavior in different frequency domains (e.g., using phonon polaritons in the infrared [13,14] or textured PCSs at lower frequencies [2,9]).

In this Letter, we introduce a new approach to systematically study surface resonances in structured PCSs. This allows us to provide further insight into recently proposed holey metamaterials [2], for which we find significant quantitative corrections in the surface mode dispersion relations. Furthermore, we show that these kinds of materials cannot be represented in general by local, frequency-dependent optical constants [$\epsilon(\omega)$ and $\mu(\omega)$], except in some limiting cases. Finally, our results suggest a new systematics in the analysis of textured PCSs that is applied to related metamaterial designs.

We shall consider a planar PCS perforated by infinitely deep square holes of side a arranged in a periodic square array of period d small compared to the wavelength λ and filled with homogeneous material of permittivity ϵ_{h} and permeability μ_{h} ($\mu_{\mathrm{h}} = 1$ will be used throughout this work), as sketched in the inset of Fig. 1(a). Pendry *et al.* [2] obtain the reflectivity of this surface by assuming that the field inside the square holes can be approximated by the lowest-frequency mode (i.e., the $\mathrm{TE}_{1,0}$ mode [15]). This allows them to describe the bulk holey material by effective local optical constants $\epsilon_{\parallel}$ and $\mu_{\parallel}$ for fields parallel to the surface and $\epsilon_{\perp} = \mu_{\perp} = \infty$ for perpendicular fields. In such a description, the reflection coefficient for p-polarized incident light (external magnetic field parallel to the surface) is given by Fresnel's equation

$$r_{\mathrm{p}} = \frac{k_z - k\sqrt{\mu_{\parallel}/\epsilon_{\parallel}}}{k_z + k\sqrt{\mu_{\parallel}/\epsilon_{\parallel}}}, \tag{1}$$

where $k = 2\pi/\lambda$ is the free-space light momentum, and $k_{\parallel}$ and $k_z = \sqrt{k^2 - k_{\parallel}^2}$ are the momentum components parallel and perpendicular to the surface, respectively. The surface resonances are signaled by the divergence of r_{p} for incident evanescent waves ($k_{\parallel} > k$), leading to

$$k_{\parallel}^2 = k^2 + \Gamma\frac{A^3 k^4}{d^4}, \tag{2}$$

with $A = a^2$ (the hole cross section) and $\Gamma = 64\mu_{\mathrm{h}}^2/\pi^6$ in the long-wavelength limit of Ref. [2]. We shall demonstrate below that a more accurate model that takes into account the effect of higher-frequency modes inside the holes still leads to an equation such as (2) but introduces important corrections in Γ and does not permit describing the holey material by local optical constants.

Figure 1 illustrates through a representative example a comparison between the model of Ref. [2] (dashed curves) and a rigorous numerical solution of Maxwell's equations obtained by expanding the electromagnetic field in terms of diffracted plane waves outside the surface and square-waveguide modes inside the holes (we find convergence using 144 waveguide modes and 400 plane waves). Our calculated results exhibit the same behavior as Eq. (2) in the long-wavelength limit [Fig. 1(a)], although, as expected, the inclusion of diffraction orders outside the ma-

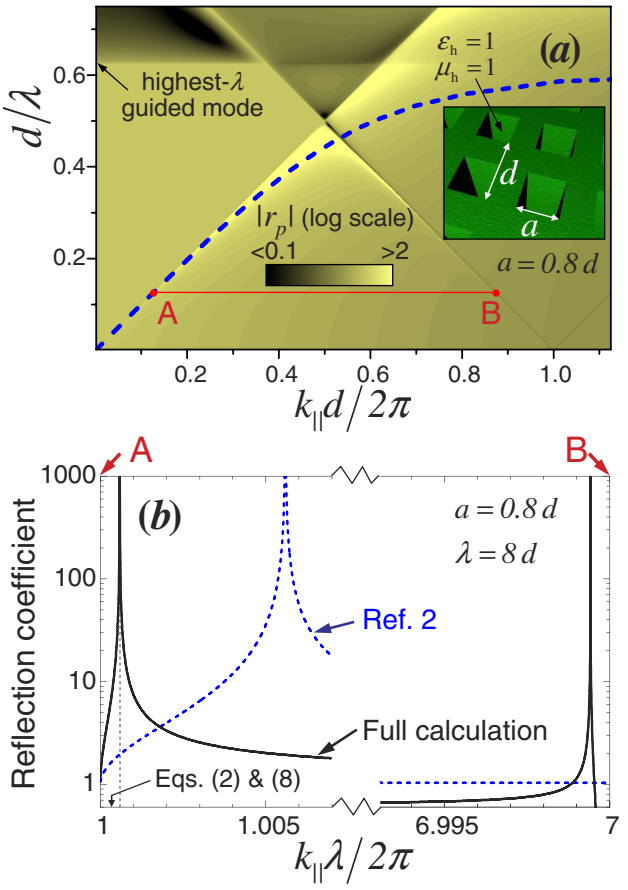

FIG. 1 (color online). (a) Modulus of the specular reflection coefficient $|r_p|$ of a perfect-conductor surface perforated by infinitely deep square holes (see inset for parameters) as a function of wavelength λ and momentum parallel to the surface $k_{||}$. The surface mode predicted in Ref. [2] is shown by a dashed curve. (b) Detail of the reflection coefficient r_p along the AB segment of (a).

terial introduces a new structure in the high-frequency region and bends the dispersion relation at the boundary of the first Brillouin zone. Closer inspection into the long-wavelength region reveals a sizable correction in the position of the resonance towards smaller values of $k_{||}$ [Fig. 1(b)], quantified in a factor of 3 larger decay length of the surface state into the vacuum. The physical origin of this discrepancy can be understood within the analytical approach that follows, corroborated by full numerical solution of Maxwell's equations.

Small holes ($a \ll d, \lambda$) can be represented by effective dipoles, as shown by Bethe [16] for a single hole in a thin perfect-conductor screen, where the scattered field is equivalent to that generated by an electric dipole perpendicular to the surface plus a parallel magnetic dipole, which are in turn proportional to the external perpendicular electric field and parallel magnetic field via the polarizabilities α_E and α_M, respectively. Parallel electric dipoles and perpendicular magnetic dipoles are forbidden by the condition that the parallel electric field and the perpendicular magnetic field vanish at a PCS. A single deep hole in a semi-infinite PCS can be described in the same fashion. In the long-wavelength limit, α_E (α_M) can be obtained from the electrostatic (magnetostatic) far field induced by an external electric (magnetic) field, as shown in Figs. 2(a) and 2(b), whose calculation involves only TM modes (TE modes) of the hole cavity. We have done this for a single square hole using the noted plane-wave expansion for arrays of holes sufficiently spaced as to neglect their mutual interaction. (We have double-checked our numerical results by independently solving the isolated hole problem.) The single circular hole has also been contemplated in Fig. 2(c), solved by using a circular wave expansion.

Now, we consider a unit p-polarized plane wave with wave vector in the xz plane (no surface modes are obtained for s polarization). The material will be contained in the $z < 0$ region. In the absence of any surface structure, the total (incident plus reflected) field reads

$$\mathbf{E}^{\text{ext}}(\mathbf{r}) = \frac{2}{k}[ik_z \sin(k_z z)\hat{\mathbf{x}} - k_{||}\cos(k_z z)\hat{\mathbf{z}}]e^{ik_{||}x},$$
$$\mathbf{H}^{\text{ext}}(\mathbf{r}) = 2\cos(k_z z)\hat{\mathbf{y}}e^{ik}. \tag{3}$$

The actual self-consistent field acting on each hole includes contributions from interhole dynamical interaction. Symmetry considerations show that the magnetic and electric dipoles describing the holes must be oriented as $\mathbf{m} = m\hat{\mathbf{y}}$ and $\mathbf{p} = p\hat{\mathbf{z}}$. Actually, $\mathbf{m}$ and $\mathbf{p}$ depend on hole positions $\mathbf{R} = (x, y)$ just through phase factors $\exp(ik_{||}x)$. This

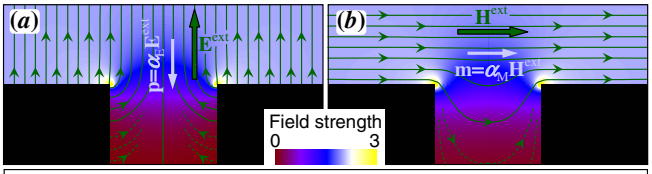

(c) $(\varepsilon_h = \mu_h = 1)$

	$\text{TE}_{1,0}$ (Ref. 2)	numerical result	numerical result	exact result
$\text{Re}\{A^{3/2}\alpha_M^{-1}\}$	$\pi^4/4 \approx 24.4$	38.1	37.3	$3\pi^{5/2}/2 \approx 26.2$
$\text{Re}\{A^{3/2}\alpha_E^{-1}\}$	∞	-61.8	-61.5	$-3\pi^{5/2} \approx -52.5$
Γ	$64/\pi^6 \approx 67\times10^{-3}$	4.0×10^{-3}	4.4×10^{-3}	$16/9\pi^3 \approx 57\times10^{-3}$

FIG. 2 (color online). (a) Electrostatic electric-field flow lines for an empty hole drilled in a semi-infinite perfect-conductor subject to an external field $\mathbf{E}^{\text{ext}}$ perpendicular to the surface, giving rise to an electric dipole $\mathbf{p} = \alpha_E\mathbf{E}^{\text{ext}}$ as seen from afar. (b) Magnetostatic magnetic-field flow lines for the same hole subject to an external parallel field $\mathbf{H}^{\text{ext}}$ and leading to a magnetic dipole $\mathbf{m} = \alpha_M\mathbf{H}^{\text{ext}}$. (c) Summary of polarizabilities for square and circular holes in PCSs, normalized using the hole area A. The circular hole in a perfect-conductor thin screen is analytical [15,16], but the right-hand side of Eq. (8) must be corrected by a factor of 4 in this case due to cooperative interaction between both sides of the film.

permits writing the self-consistent relations [5]

$$p = \alpha_{\mathrm{E}}[E_z^{\mathrm{ext}} + G_{zz}^{\mathrm{EE}} p + G_{zy}^{\mathrm{EM}} m],$$
$$m = \alpha_{\mathrm{M}}[H_y^{\mathrm{ext}} + G_{yy}^{\mathrm{MM}} m + G_{yz}^{\mathrm{ME}} p], \tag{4}$$

where $G_{ij}^{\nu\nu'}$ gives the i component of the electric ($\nu = \mathrm{E}$) or magnetic ($\nu = \mathrm{M}$) field induced at the position of a central hole by the j component of the electric ($\nu' = \mathrm{E}$) or magnetic ($\nu' = \mathrm{M}$) dipoles of the rest of the holes. This coefficients satisfy the symmetry relations $G_{ij}^{\mathrm{EE}} = G_{ij}^{\mathrm{MM}}$ and $G_{ij}^{\mathrm{EM}} = -G_{ij}^{\mathrm{ME}} = -G_{ji}^{\mathrm{EM}}$, where i and j denote y or z Cartesian components, and they are defined as sums over hole lattice sites $\mathbf{R}$. More precisely,

$$G_{ij}^{\mathrm{EE}} = \sum_{\mathbf{R}\neq\mathbf{0}} e^{-ik_{\parallel}x} e(k^2 + \partial_i\partial_j)\frac{e^{ikR}}{R},$$
$$G_{yz}^{\mathrm{EM}} = -ik\sum_{\mathbf{R}\neq\mathbf{0}} e^{-ik_{\parallel}x}\partial_x\frac{e^{ikR}}{R}. \tag{5}$$

This interhole interaction is generally small for $a \ll d$, except when a diffraction order goes grazing, in which case the above sums can diverge giving rise to phenomena related to Wood's anomalies [17]. It is near these divergences that surface-bound modes can exist, subject to the condition

$$(\alpha_{\mathrm{E}}^{-1} - G_{zz}^{\mathrm{EE}})(\alpha_{\mathrm{M}}^{-1} - G_{yy}^{\mathrm{EE}}) = (G_{yz}^{\mathrm{EM}})^2, \tag{6}$$

which guarantees the existence of nonvanishing solutions of Eq. (4) in the absence of external fields. In particular, near the light line in the $k_{\parallel} - k$ plane for $k_{\parallel} > k$, one has

$$\mathrm{Re}\{G_{zz}^{\mathrm{EE}}\} \approx \mathrm{Re}\{G_{yy}^{\mathrm{EE}}\} \approx \mathrm{Re}\{G_{yz}^{\mathrm{EM}}\} \approx \frac{2\pi i k^2}{k_z d^2} \equiv S, \tag{7}$$

which comes from the divergent terms of Eq. (5) when they are recast as sums over reciprocal space [see Fig. 3(a)]. Furthermore, upon inspection, one finds that $\mathrm{Im}\{G_{yz}^{\mathrm{EM}}\} = 0$, and the remaining imaginary parts of all quantities in Eq. (6) cancel out exactly since $\mathrm{Im}\{G_{jj}^{\mathrm{EE}}\} = \mathrm{Im}\{\alpha_{\nu}^{-1}\} = -2k^3/3$ (this exact formula follows from instantaneous flux conservation for $k_{\parallel} > k$). Combining these results, Eq. (6) can be approximated by Eq. (2) with

$$\Gamma = \frac{4\pi^2}{A^3}\left(\frac{1}{\mathrm{Re}\{\alpha_{\mathrm{E}}^{-1}\}} + \frac{1}{\mathrm{Re}\{\alpha_{\mathrm{M}}^{-1}\}}\right)^2. \tag{8}$$

Equation (8) is exact in the $a \ll d \ll \lambda$ limit, and it predicts the existence of surface-bound modes under the condition $1/\mathrm{Re}\{\alpha_{\mathrm{E}}^{-1}\} + 1/\mathrm{Re}\{\alpha_{\mathrm{M}}^{-1}\} > 0$. Calculated values of Γ are offered in Fig. 2(c) for various hole geometries. The position of the surface mode calculated from Eq. (8) [see Fig. 1(b)] differs slightly from the exact numerical result, mainly due to neighboring-holes multipolar interaction for $a = 0.8d$ (the holes occupy 64% of the surface).

Interestingly, circular and square holes of the same area give rise to similar values of Γ. This parameter increases by an order of magnitude when the holes are made on thin screens, as compared to deep holes [last column in Fig. 2(c)], giving rise to surface modes that are farther apart from the light line due to cooperative interaction between both sides of the film.

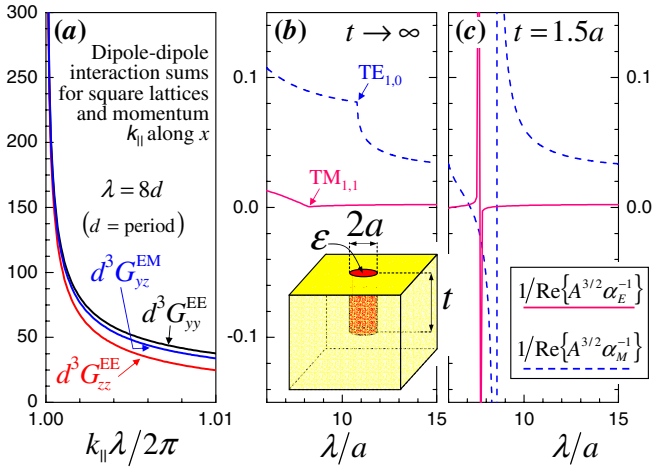

FIG. 3 (color online). (a) Real part of the dipole-dipole interaction sums for a square lattice of period d [Eq. (5) for $k_{\parallel} \gtrsim k$]. (b) Electric (solid curve) and magnetic (dashed curve) polarizabilities of single circular holes filled with $\epsilon_{\mathrm{h}} = 10$ material as a function of hole size. (c) Same as (b) for dimples.

This description in terms of effective dipoles permits writing the specular reflection coefficient for p-polarized light as $r_{\mathrm{p}} = 1 + S(m - pk_{\parallel}/k)$. It is easy to see that this expression does not conform in general to the assumption of local optical constants implicit in the derivation of Eq. (1). In particular, for nongrazing incidence and $\lambda \gg d$, the dipole-dipole interaction can be neglected in Eq. (4), so that using explicit expressions for the fields as provided by Eq. (3), and noticing the r_{p} deviates only slightly from unity under these conditions, one finds, upon comparison with Eq. (1),

$$\sqrt{\mu_{\parallel}/\epsilon_{\parallel}} \approx \frac{2\pi i k}{d^2}[\alpha_{\mathrm{M}} + (k_{\parallel}/k)^2\alpha_{\mathrm{E}}], \tag{9}$$

which depends on $k_{\parallel}$ (i.e., on the angle of incidence) unless $\alpha_{\mathrm{E}} = 0$. Thus, the metamaterial is nonlocal in general, so that the optical constants of an equivalent homogeneous medium will depend on both frequency and momentum (spatial dispersion). It should be noted that the neglect of cavity modes other than the lowest-frequency one ($\mathrm{TE}_{1,0}$), as assumed in Ref. [2], yields $\alpha_{\mathrm{E}} = 0$ [see Fig. 2(c)], and therefore it leads to an incomplete local-response description of the metamaterial.

From the point of view of external fields, the local-response picture will be still maintained if $|\alpha_{\mathrm{E}}| \ll |\alpha_{\mathrm{M}}|$, so that the second term on the right-hand side of Eq. (9) can be overlooked. Such metamaterials can be achieved by filling the holes with media of very high $|\epsilon_{\mathrm{h}}| \gg 1$ or alternatively by using specific electrostatic resonances in the $-1 < \epsilon_{\mathrm{h}} < 0$ range (piling up towards $\epsilon_{\mathrm{h}} = -1$ as a

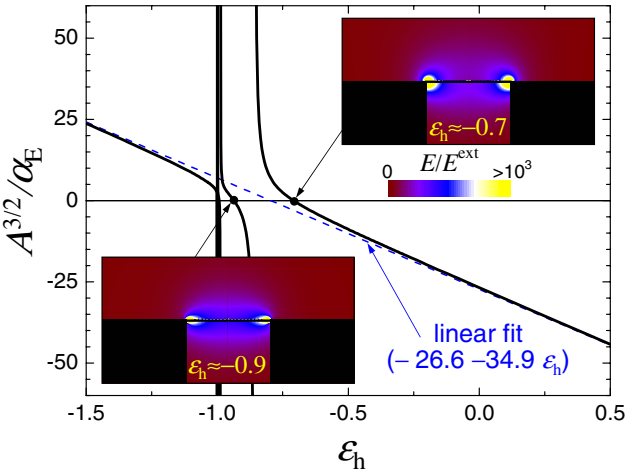

FIG. 4 (color online). Inverse of the electrostatic polarizability of a single circular hole of area A as a function of the dielectric constant ϵ_h of the filling material. The field strength distribution is shown in the insets for the two lowest-order resonances in the $-1 < \epsilon_h < 0$ range. The magnetostatic response is independent of $\epsilon_h (A^{3/2}/\alpha_M \approx 37.3)$.

manifestation of their filling-material surface-plasmon origin). This can make α_E negligible in the long-wavelength limit, as shown in Fig. 4. Optical phonons in alkali halides yield $\epsilon_h \approx -1$ with small absorption and can be combined with noble metals (near-perfect conductors) to implement these ideas in the THz domain.

Another possibility consists in filling dimples rather than holes using moderate values of $\epsilon_h > 1$ and λ/d. Indeed, the high-frequency propagating modes of infinitely deep holes become resonances of finite width (due to coupling to the external continuum) in holes of finite depth (dimples), which are blueshifted with respect to the noted propagating modes owing to reflection at the bottom and top ends of the hole (Fabry-Perot picture), as illustrated by comparing Figs. 3(b) and 3(c). For the choice of parameters of Fig. 3(c), there is a resonance in α_M near the lowest-frequency cavity mode ($\lambda = 7.2a$), where α_E is comparatively negligible.

It should be noted that the surface modes resemble surface plasmons not only in their limited penetration into the vacuum, but also in the interaction that they provide between additional surface features like holes of larger dimensions. Indeed, the scattered field produced by one of such features in the metamaterial decays away along the surface as $\exp(ik_\parallel R)/\sqrt{R}$ at large distance R. This has the same form as the charge distribution accompanying a surface plasmon launched by a localized source, in contrast to the $\exp(ikR)/R$ far-field dependence of the interaction on unstructured PCSs [flux conservation in 2D (3D) entails the $1/\sqrt{R}$ $(1/R)$ dependence]. Furthermore, the far field of a small, localized additional surface feature can be assimilated to the field of an effective dipole placed at the surface of an equivalent homogeneous material with the same reflectivity as the holey metamaterial. Interestingly, in contrast to the dipoles that describe the underlying hole structure, the new effective dipole can have parallel electric and perpendicular magnetic components. This introduces another handle in the design of surface states by using the above holey metamaterials as the base fabric to build metamaterials drilled by larger holes, allowing us to speculate on surface modes in fractal structures that imitate Sierpinski's carpet.

In conclusion, we have introduced a formalism to study textured perfect-conductor surfaces that allows us to obtain quasianalytical long-wavelength exact dispersion relations for surface-bound modes. We have found that these metamaterials cannot be assimilated in general to equivalent effective homogeneous media described by local optical constants, except in some limiting cases (e.g., by filling the holes with high index of refraction material). Finally, our results pave the way towards simple analysis of new metamaterial designs based upon the coexistence of different hole sizes and hole distributions that can realize the goal of achieving on-demand tailored surface dispersion relations.

F. J. G. A. would like to thank Professor Pendry for helpful suggestions and for very enjoyable and stimulating discussions. This work was supported in part by the Spanish MEC (FIS2004-06490-C03-02 and BFM2003-01167) and by the European Commission (*Metamorphose* NoE NMP3-CT-2004-500252 and *Molecular Imaging* IP LSHG-CT-2003-503259).

*Corresponding author.
Electronic address: jga@sw.ehu.es

[1] T. W. Ebbesen *et al.*, Nature (London) **391**, 667 (1998).
[2] J. B. Pendry *et al.*, Science **305**, 847 (2004).
[3] R. H. Ritchie, Phys. Rev. **106**, 874 (1957).
[4] R. Gordon *et al.*, Phys. Rev. Lett. **92**, 037401 (2004).
[5] R. E. Collin and W. H. Eggimann, IEEE Trans. Microwave Theory Tech. **9**, 110 (1961); C. C. Chen, IEEE Trans. Microwave Theory Tech. **19**, 475 (1971).
[6] R. C. McPhedran *et al.*, in *Electromagnetic Theory of Gratings*, edited by R. Petit (Springer-Verlag, Berlin, 1980), p. 227.
[7] J. Gómez Rivas *et al.*, Phys. Rev. B **68**, 201306(R) (2003).
[8] H. Cao and A. Nahata, Opt. Express **12**, 1004 (2004).
[9] A. P. Hibbins *et al.*, Science **308**, 670 (2005).
[10] S. C. Schuster *et al.*, Nature (London) **365**, 343 (1993).
[11] W. L. Barnes *et al.*, Nature (London) **424**, 824 (2003).
[12] R. Colombelli *et al.*, Science **302**, 1374 (2003).
[13] J.-J. Greffet *et al.*, Nature (London) **416**, 61 (2002).
[14] R. Hillenbrand *et al.*, Nature (London) **418**, 159 (2002).
[15] J. D. Jackson, *Classical Electrodynamics* (Wiley, New York, 1975).
[16] H. A. Bethe, Phys. Rev. **66**, 163 (1944).
[17] R. W. Wood, Phys. Rev. **48**, 928 (1935).